J Mater Sci (2010) 45:5347–5352
DOI 10.1007/s10853-010-4583-4

Controllable synthesis and magnetic properties of Fe_3O_4 and $Fe_3O_4@SiO_2$ microspheres

Yang Cheng · Ruiqin Tan · Weiyan Wang · Yanqun Guo · Ping Cui · Weijie Song

Received: 25 February 2010 / Accepted: 29 April 2010 / Published online: 14 May 2010

Abstract We present a systematic study on the preparation, microstructure, and magnetic properties of Fe_3O_4 microspheres and $Fe_3O_4@SiO_2$ microspheres. Results showed that Fe_3O_4 microspheres' diameter can be tuned by Fe^{3+} concentration, whereas their average grain size can be tuned by polyethylene glycol (PEG) 2000 dosage or PEG molecular weight. The magnetic saturation value of Fe_3O_4 microspheres was observed to be dependent on their average grain size, but not the sphere diameter. $Fe_3O_4@SiO_2$ microspheres with different magnetic saturation values were achieved by adjusting shell thickness. Furthermore, the synthesized Fe_3O_4 and $Fe_3O_4@SiO_2$ microspheres with high and controllable magnetic saturation value endow them with great application potentials.

Introduction

Magnetic microspheres and magnetic core–shell structures are of great interest to research for their potential applications in bio and environmental fields [1–6]. $Fe_3O_4@SiO_2$ magnetic microspheres, consisting of an iron oxide core and silica shell, have attracted particular attention in bioseparation, enzyme immobilization, and diagnostic, attributed to unique magnetic responsivity, low cytotoxicity, and chemically modifiable surface [7–17].

Y. Cheng · W. Wang · Y. Guo · P. Cui · W. Song (✉)
Ningbo Institute of Material Technology and Engineering, Chinese Academy of Sciences, Ningbo 315201, People's Republic of China
e-mail: weijiesong@nimte.ac.cn

R. Tan
College of Information Science and Engineering, Ningbo University, Ningbo 315211, People's Republic of China

Up to now, several papers have been reported about the synthesis of Fe_3O_4 and $Fe_3O_4@SiO_2$ microspheres. In the early stage, Fe_3O_4 superparamagnetic crystals sized in of $\sim$10 nm were genetically encapsulated by silica shell with thickness in the range 20–100 nm [18–22]. However, the magnetic saturation value of $Fe_3O_4@SiO_2$ microspheres decreased sharply after silica shell enveloping due to the low Fe_3O_4 mass fraction [18–22], which restricted the application of $Fe_3O_4@SiO_2$ microspheres as functional materials. Recently, Fe_3O_4 polycrystal microspheres composed of small nanoparticles were successfully prepared by solvothermal method [8]. The as-prepared Fe_3O_4 microspheres possessed large diameter (200–800 nm) and high magnetic saturation value ($\sim$80 emu/g). Moreover, when the Fe_3O_4 microspheres were enveloped with silica shell, the $Fe_3O_4@SiO_2$ core–shell microspheres still retained high magnetic saturation value [23]. These results largely expanded the application potentials of $Fe_3O_4@SiO_2$ microspheres [23–25]. Further investigation on the relationship between microstructure and magnetic properties of the Fe_3O_4 and $Fe_3O_4@SiO_2$ microspheres is necessary for their applications in various fields.

In this paper, Fe_3O_4 and $Fe_3O_4@SiO_2$ microspheres with different diameters and average grain sizes were synthesized, their magnetic properties were presented, and the relationship between the microstructures and magnetic properties was discussed.

Experimental

Preparation

All the reagents used were of analytical grade. Fe_3O_4 microspheres were synthesized by modified reduction

Table 1 Reagents used in the synthesis of Fe_3O_4 microspheres: (a) different dosages of $FeCl_3{\cdot}6H_2O$; (b) different dosages of PEG 2000; (c) different molecular weights of PEG

a		b		c	
PEG 2000 (g)	$FeCl_3{\cdot}6H_2O$ (g)	PEG 2000 (g)	$FeCl_3{\cdot}6H_2O$ (g)	PEG molecular weight	$FeCl_3{\cdot}6H_2O$ (g)
2	2.70	1	2.70	200	2.70
2	5.40	2	2.70	400	2.70
2	8.10	3	2.70	600	2.70
		4	2.70	1000	2.70
		5	2.70	2000	2.70
		6	2.70	10000	2.70
				20000	2.70

reaction between $FeCl_3$ and ethylene glycol (EG) in a solvothermal system [8]. Firstly, $FeCl_3{\cdot}6H_2O$ (2.70–8.10 g) was dissolved in 80 mL EG to form an orange solution. Various Fe^{3+} concentrations (Table 1a) were used in our experiments. Subsequently, NaAc (3.6 g) and polyethylene glycol (PEG) were added, followed by vigorously stirring for 30 min. Herein, PEG 2000 with various dosages from 1.0 to 6.0 g (Table 1b) or PEG with various molecular weights from 200 to 20000 (Table 1c) was introduced. Afterward, the mixture was sealed in a Teflon-lined stainless steel autoclave and maintained at 473 K for 8 h before cooling to room temperature. Finally, the black powder was rinsed with ethanol for several times and dried at 333 K for 6 h.

SiO_2 shells were coated on the synthesized Fe_3O_4 microspheres through hydrolysis and condensation of tetraethylorthosilicate (TEOS) in a mixture of isopropyl alcohol, water, and ammonia [26]. Firstly, as-prepared Fe_3O_4 powder (0.3 g) was added to a solution of 0.75 mL aqueous ammonia (30 wt%) and 5.5 mL water in 100 mL isopropyl alcohol, followed by stirring at room temperature for 30 min. Afterward, TEOS (0.2–0.8 mL) was quickly added, and then maintained at room temperature for 12 h. Finally, the $Fe_3O_4@SiO_2$ microspheres were rinsed with ethanol for several times at room temperature, and dried at 333 K for 6 h. It should be mentioned that the difference in TEOS dosage resulted in different silica shell thicknesses.

Characterization

X-ray diffraction (XRD) analysis was carried out using a Bruker AXS D8 advance diffractometer with Cu Kα radiation at a power of 1.6 kW. All diffraction patterns were calibrated using the standard spectra of corundum. The grain size was calculated using the Scherrer equation $D = K\lambda/\beta \cos\theta$ [27], where β was the width of the XRD peak at half height, θ was the angle, λ was the X-ray wave length (1.54 Å), and K was a shape factor, about 0.89 for magnetite. The morphology and microstructure of the microspheres were characterized by a Hitachi S-4800 field emission scanning electron microscope and a FEI Tecnai G2 F20 field emission transmission electron microscope, respectively. Magnetic properties of the microspheres were conducted using a Lakeshore 7400 vibrating sample magnetometer (VSM).

Results and discussion

Diameter and magnetic properties of Fe_3O_4 microspheres

Figure 1 shows the representative SEM images of Fe_3O_4 microspheres synthesized with different Fe^{3+} concentrations. It was observed that, in each case, Fe_3O_4 microspheres were composed of small nanoparticles, whereas their diameter increased with induced $FeCl_3{\cdot}6H_2O$ dosage, which was of $\sim$200 nm at $FeCl_3{\cdot}6H_2O$ dosage of 2.7 g (Fig. 1a), $\sim$400 nm at 5.4 g (Fig. 1b), and $\sim$600 nm at 8.1 g (Fig. 1c). To further verify the microstructure of Fe_3O_4 microspheres, TEM image of Fe_3O_4 microspheres sized in $\sim$400 nm is shown in Fig. 2a, the SAED image is in the inset of Fig. 2a. It was revealed that the Fe_3O_4 microspheres were polycrystalline in nature, which was in accordance with the previous results [3, 15, 24]. Moreover, the high-resolution TEM image of the box region of Fig. 2a further supported the polycrystalline nature of the synthesized microspheres, as shown in Fig. 2b. The interlayer distances were calculated to be $\sim$0.48 and $\sim$0.30 nm, which agree well with the separation between the (111) and (220) lattice planes, respectively. Figure 3 shows the XRD patterns of the same Fe_3O_4 microspheres in Fig. 1. It can be observed that under each circumstance, the diffraction peaks related to Fe_3O_4 structure were the same and, moreover, the average grain size of Fe_3O_4 microspheres estimated from XRD peak (311) was of $\sim$20 nm.

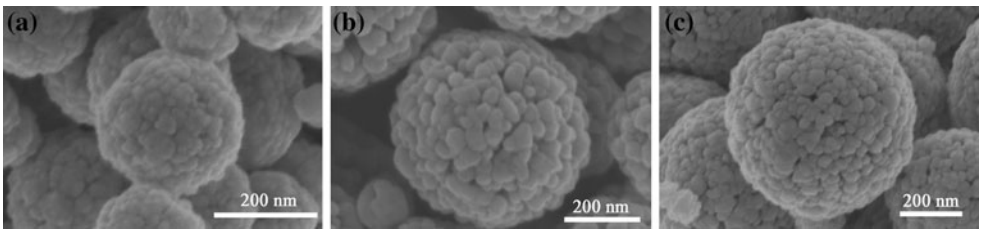

Fig. 1 Representative SEM images of Fe_3O_4 microspheres synthesized with different amounts of $FeCl_3 \cdot 6H_2O$ in 80 mL EG. **a** 2.7 g; **b** 5.4 g; **c** 8.1 g

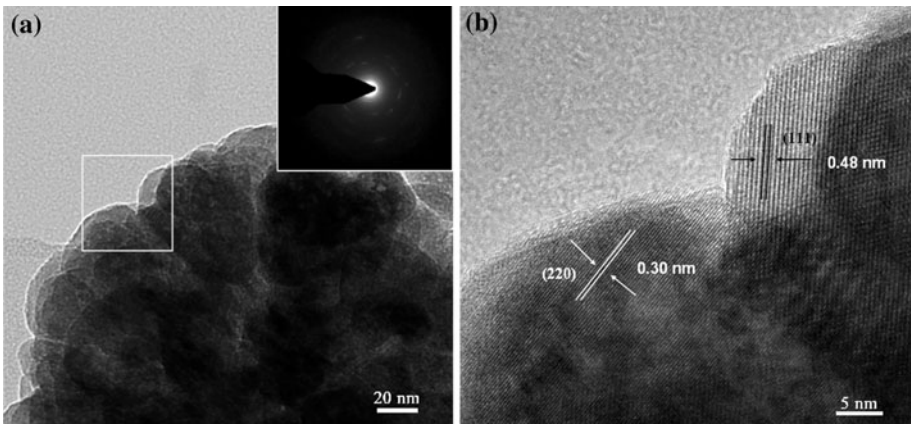

Fig. 2 **a** TEM and SAED images of 400 nm Fe_3O_4 microspheres; **b** HRTEM image of the boxed region of part (**a**)

Therefore, it can be concluded that the diameter of Fe_3O_4 microspheres increased with Fe^{3+} concentration, whereas the average grain size of Fe_3O_4 microspheres was irrespective of Fe^{3+} concentration. Here larger amount of Fe_3O_4 nanoparticles can be formed with the increase in Fe^{3+} concentration, leading to the larger diameter of Fe_3O_4 microspheres, whereas the average grain size of Fe_3O_4 microspheres is supposed to be related to surfactant, which is the same in this set of samples (2 g PEG 2000). It should be mentioned that the diameter of Fe_3O_4 microspheres is believed to be large enough to further prepare $Fe_3O_4@SiO_2$ microspheres with high magnetic saturation value, as reported by Deng et al. [3, 24]. The magnetic properties of $Fe_3O_4@SiO_2$ microspheres discussed in the "Effect of $Fe_3O_4@SiO_2$ microsphere shell thickness on magnetic properties" section.

Furthermore, the effect of microsphere diameter on the magnetic properties of Fe_3O_4 microspheres was investigated using VSM. Figure 4 shows the magnetic hysteresis loops of the same Fe_3O_4 microspheres in Fig. 1. It was observed that the magnetic saturation value or coercive force of Fe_3O_4 microspheres was irrespective of Fe_3O_4 microspheres diameter, which was of $\sim$82.0 emu/g and $\sim$100 Oe, respectively, indicating that the magnetic properties of Fe_3O_4 microspheres were mainly determined by the average grain size, but not the sphere diameter.

Grain size and magnetic properties of Fe_3O_4 microspheres

As mentioned above, the average grain size of Fe_3O_4 microspheres is supposed to be related to surfactant. Accordingly, PEG 2000 with different dosages from 1 to 6 g (Table 1b), or 1 g PEG with different molecular weights from 200 to 20000 (Table 1c) was added during the synthesis of Fe_3O_4 microspheres. The XRD patterns of Fe_3O_4 microspheres synthesized with each above-mentioned PEG exhibited the same diffraction peaks as these of the samples shown in Fig. 3, whereas the average grain size of Fe_3O_4 microspheres estimated from XRD peak (311) changed with the dosage of PEG 2000 or molecular weight of PEG, as shown in Fig. 5.

As illustrated in Fig. 5a, the average grain size of Fe_3O_4 microspheres decreased from 20.3 to 17.6 nm with the increase in PEG 2000 dosage from 1 to 6 g and, moreover, the average grain size did not significantly decrease any more as the PEG 2000 dosage exceeding 4 g. The SEM images of Fe_3O_4 microspheres synthesized with 2 and 6 g PEG 2000 are shown in Fig. 6, indicating the grain size of Fe_3O_4 microspheres decreased from $\sim$20 to $\sim$15 nm with the increase in PEG 2000 dosage. Obviously, the density of PEG 2000 immobilizing on Fe_3O_4 nanocrystals increases with PEG 2000 dosage, leading to the smaller grain size of Fe_3O_4 microspheres. Furthermore, the grain size does not

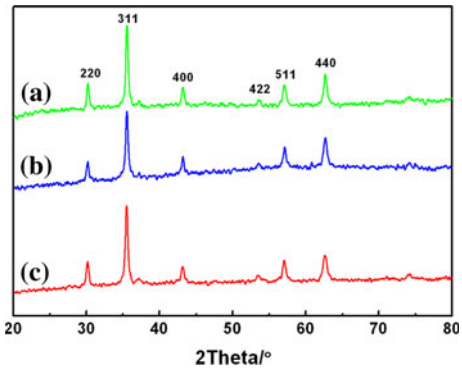

Fig. 3 XRD patterns of Fe_3O_4 microspheres with different diameters. **a** 200 nm; **b** 400 nm; **c** 600 nm

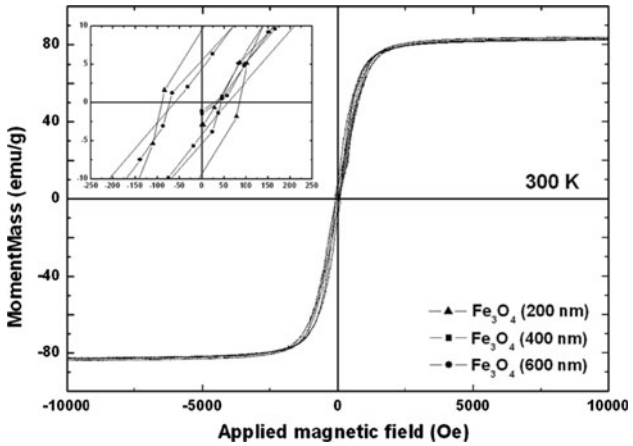

Fig. 4 Magnetic hysteresis loops of 200/400/600 nm Fe_3O_4 microspheres. Inset image is the low magnetic field region of magnetic hysteresis loops

markedly decrease any more as the saturation density of PEG 2000 covering on Fe_3O_4 nanocrystals achieves, which is of 4 g PEG 2000 in our result.

On the other hand, as shown in Fig. 5b, larger average grain size of Fe_3O_4 microspheres can be obtained when either smaller (200–1000) or larger (10000–20000) molecular weight of PEG was used. In contrast, smaller average grain size of Fe_3O_4 microspheres formed when PEG with medium molecular weight (2000) was used, which was in accordance with the previous results of Au nanoparticles synthesized by different PEG molecular weight [28]. It is supposed that PEG with molecular weight in the range 200–1000 is not sufficient to limit the Fe_3O_4 nanocrystals, as a result, Fe_3O_4 nanocrystals tend to form larger cluster by fusing together, leading to the large grain size of Fe_3O_4 microspheres. As soon as the molecular weight of PEG exceeds 2000, one PEG chain enough limits Fe_3O_4 nanocrystals; therefore, the grain size of Fe_3O_4 microspheres increases with the molecular weight of PEG.

Furthermore, the effect of grain size on the magnetic properties of Fe_3O_4 microspheres is investigated. Figure 7 shows the magnetic hysteresis loops of Fe_3O_4 microspheres with different grain sizes. It was observed that the magnetic saturation value of Fe_3O_4 microspheres changed from ~70 to ~80 emu/g when the average grain size of Fe_3O_4 microspheres altered in the range 17.8–23.5 nm and, moreover, the highest magnetic saturation value was obtained when the average grain size was 20.7 nm, which was supposed to be attributed to the most suitable grain size for magnetic response ability. Similar results have also been proposed by Wang et al. [28]. Also, it was observed that the coercive forces of Fe_3O_4 microspheres only increased from ~12 Oe to ~40 Oe with the increase in the grain size from 17.8 to 23.5 nm, suggesting relative low coercive force value of Fe_3O_4 microspheres with average grain size in the range 17.8–23.5 nm.

Effect of Fe_3O_4@SiO_2 microsphere shell thickness on magnetic properties

Recently, Fe_3O_4@SiO_2 core–shell microspheres have attracted particular attentions in various fields, due to its unique magnetic responsivity, low cytotoxicity, and chemically modifiable surface. Whereas relatively poor magnetic response limits their application potentials. Accordingly, preparation of Fe_3O_4@SiO_2 microspheres with large magnetic saturation value has been intensively investigated. Herein, choosing ~400 nm Fe_3O_4 microspheres with average grain size of ~20 nm, a series of Fe_3O_4@SiO_2 core–shell microspheres with different shell

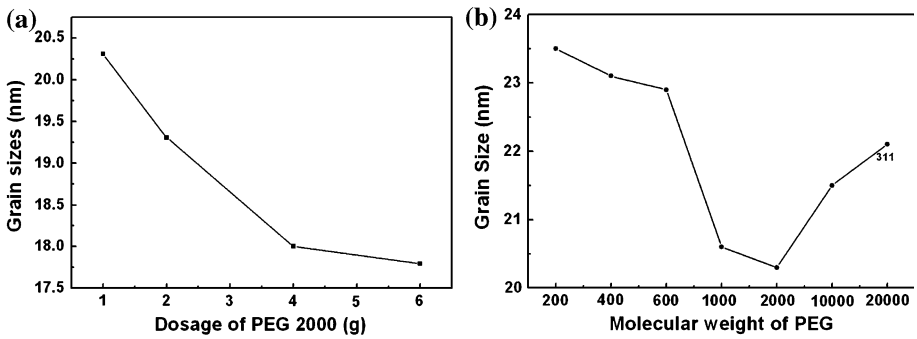

Fig. 5 Dependence of grain size of Fe_3O_4 microspheres on **a** PEG 2000 dosage; **b** PEG molecular weight

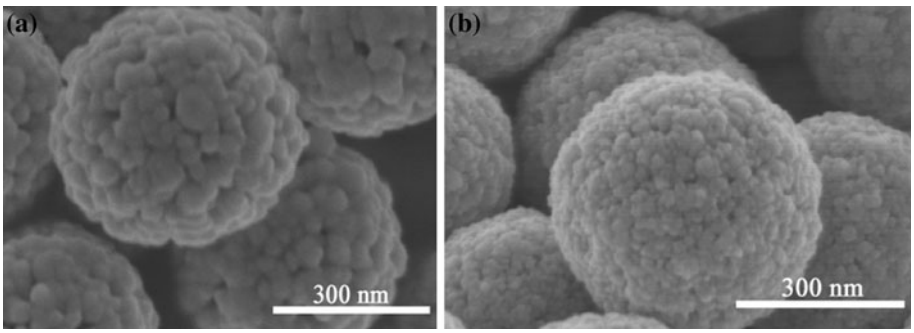

Fig. 6 SEM images of 400 nm Fe_3O_4 microspheres synthesized with different dosages of PEG 2000. **a** 2 g; **b** 6 g

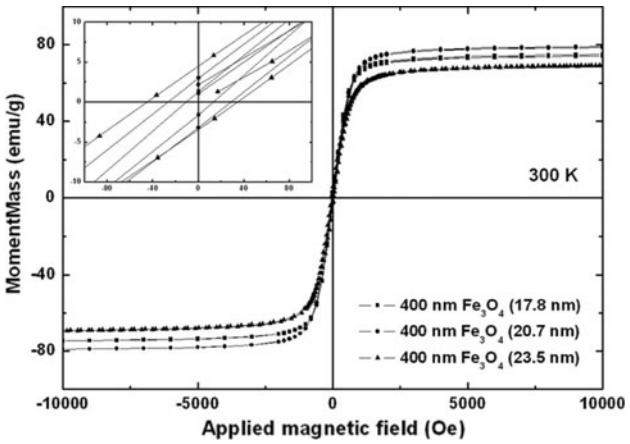

Fig. 7 Magnetic hysteresis loops of 400 nm Fe_3O_4 microspheres with different grain sizes. Inset image is the low magnetic field region of magnetic hysteresis loops

thicknesses have been obtained. Figure 8 shows SEM images of $Fe_3O_4@SiO_2$ microspheres with different dosages of TEOS, the cross-sectional images shown in Fig. 8d–f were taken from the broken core–shell microspheres. It was observed that the shell thickness increased from ~50 to ~200 nm as the TEOS dosage increased from 0.2 to 0.8 mL and, moreover, smooth $Fe_3O_4@SiO_2$ microsphere surface was obtained in each case, which accorded with the demands for application as functional magnetic carriers.

Figure 9 shows the magnetic hysteresis loops of the above-mentioned $Fe_3O_4@SiO_2$ microspheres. It was observed that the magnetic saturation values of $Fe_3O_4@SiO_2$ microspheres decreased from ~74.5 to ~52.5 emu/g when the shell thicknesses increased from ~50 to ~200 nm. Therefore, on one hand, it is revealed that the magnetic saturation value of synthesized $Fe_3O_4@SiO_2$ microspheres was significantly enhanced compared to the traditional $Fe_3O_4@SiO_2$ microspheres with magnetic saturation value in the range 10–20 emu/g. The reason for which is ascribed to that the diameter of our Fe_3O_4 microspheres is much larger than that of traditional Fe_3O_4 nanocrystals (~10 nm); on the other hand, controlled magnetic saturation values of $Fe_3O_4@SiO_2$ microspheres can be obtained by changing shell thickness, resulting in that the synthesized $Fe_3O_4@SiO_2$ microspheres can cover wide applications with demands of various magnetic saturation value. Moreover, the coercive force slightly increased from ~40 Oe to ~100 Oe with the increase in shell thickness from ~50 to ~200 nm. $Fe_3O_4@SiO_2$ microspheres with coercive force value lower than ~100 Oe does not influence their disperssional performance in solution remarkably.

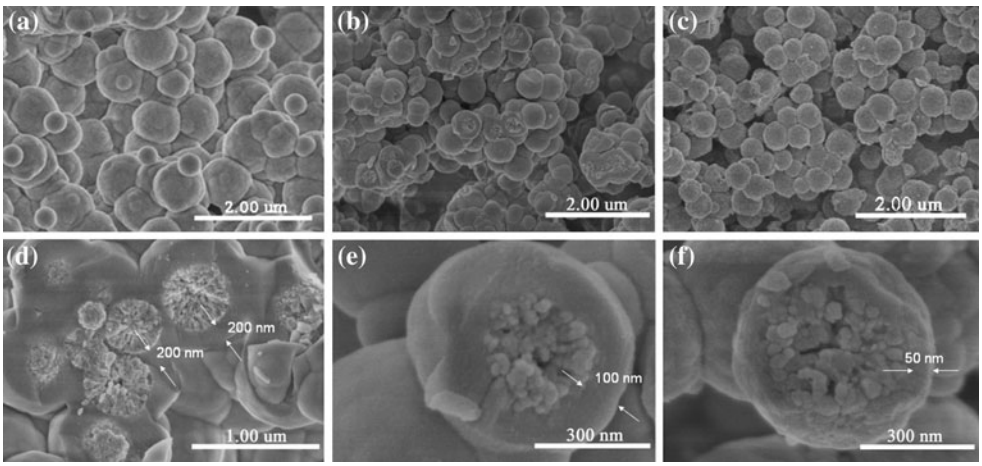

Fig. 8 SEM images of $Fe_3O_4@SiO_2$ microspheres with different dosages of TEOS. **a**, **d** 0.8 mL; **b**, **e** 0.3 mL; **c**, **f** 0.2 mL

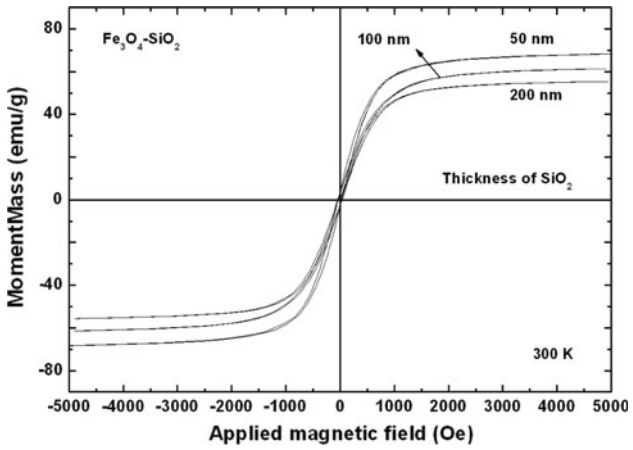

Fig. 9 Magnetic hysteresis loops of Fe_3O_4@SiO_2 core–shell microspheres with different shell thicknesses

Conclusion

Fe_3O_4 microspheres with various diameter and grain size were successfully synthesized in this study. It was observed that the microspheres were composed of small nanoparticles and polycrystalline in nature. The diameter of Fe_3O_4 microspheres was adjusted from $\sim$200 to $\sim$600 nm by increasing Fe^{3+} concentration, and the average grain size of Fe_3O_4 microspheres was adjusted by using different dosage of PEG 2000 or different molecular weight of PEG. The magnetic saturation value of Fe_3O_4 microspheres was determined by the average grain size but not the sphere diameter. The magnetic saturation value of the Fe_3O_4@SiO_2 microspheres decreased from $\sim$74.5 to $\sim$52.5 emu/g when the shell thickness increased from $\sim$50 to $\sim$200 nm. The Fe_3O_4 and Fe_3O_4@SiO_2 microspheres with high and controllable magnetic saturation value may create novel applications in functional nanostructures.

Acknowledgement The authors appreciate the financial support of the "Hundred Talents Program," the Chinese Academy of Sciences, the Natural Science Foundation of China (29075107), the Zhejiang Natural Science Foundation (Y407364), and the Ningbo Natural Science Foundation (2008A610047, 2009A610018).

References

1. Chan Y, Zimmer JP, Stroh M, Steckel JS, Jain RK, Bawendi MG (2004) Adv Mater 16:2092
2. Breen ML, Dinsmore AD, Pink RH, Qadri SB, Ratna BR (2001) Langmuir 17:903
3. Deng YH, Yang WL, Wang CC, Fu SK (2003) Adv Mater 15:1729
4. Von-Werne T, Patten TE (1999) J Am Chem Soc 121:7409
5. Salgueiriño-Maceira V, Correa-Duarte MA, Spasova M, Liz-Marzán LM, Farle M (2006) Adv Mater 16:509
6. Caruso F, Susha AS, Giersig M, Möhwald H (1999) Adv Mater 11:950
7. Tripp SL, Pusztay SV, Ribbe AE, Wei A (2002) J Am Chem Soc 124:7914
8. Deng H, Li X, Peng Q, Wang X, Chen J, Li Y (2005) Angew Chem Int Ed 44:2782
9. Rabani E, Reichman DR, Geissler PL, Brus LE (2003) Nature 426:271
10. Ulman A (1996) Chem Rev 96:1533
11. Hu HB, Wang ZH, Pan L (2010) J Alloys Compd 492:656
12. Luo B, Song XJ, Zhang F et al (2010) Langmuir 26:1674
13. Wu W, Xiao XH, Zhang SF et al (2010) Nanoscale Res Lett 5:116
14. Tan H, Xue JM, Shuter B et al (2010) Adv Funct Mater 20:722
15. Chen HM, Deng CH, Zhang XM (2010) Angew Chem Int Ed 49:607
16. Xu Y, Karmakar A, Wang DY et al (2010) J Phys Chem C 114:5020
17. Chen HM, Lu XH, Deng CH et al (2009) J Phys Chem C 113:21068
18. Kim J, Lee JE, Lee J, Yu JH, Kim BC, An K, Hwang Y, Shin CH, Park JG, Kim J, Hyeon T (2006) J Am Chem Soc 128:688
19. Lin YS, Wu SH, Hung Y, Chou YH, Chang C, Lin ML, Tsai CP, Mou CY (2006) Chem Mater 18:5170
20. Giri S, Trewyn BG, Stellmaker MP, Lin VSY (2005) Angew Chem Int Ed 44:5038
21. Zhao WR, Gu JL, Zhang LX, Chen HR, Shi JL (2005) J Am Chem Soc 127:8916
22. Du BY, Mei AX, Tao PJ, Zhao B, Cao Z, Nie JJ, Xu JT, Fan ZQ (2009) J Phys Chem C 113:10090
23. Xu XQ, Deng CH, Gao MX, Yu WJ, Yang PY, Zhang XM (2006) Adv Mater 18:3289
24. Deng YH, Qi DW, Deng CH, Zhang XM, Zhao DY (2008) J Am Chem Soc 130:28
25. Jia BP, Gao L (2007) Scr Mater 56:677
26. Stöber W, Fink A, Bohn E (1968) J Colloid Interface Sci 26:62
27. Sun J, Zhou S et al (2007) J Biomed Mater Res A 80A(2):333
28. Wang CH, Liu CJ, Wang CL et al (2008) J Phys D Appl Phys 41:195301